

MIT Open Access Articles

*Comparison of Inverter Topologies for
High-Speed Motor Drive Applications*

The MIT Faculty has made this article openly available. **Please share** how this access benefits you. Your story matters.

Citation: Qasim, Mohammad and Perreault, David. 2021. "Comparison of Inverter Topologies for High-Speed Motor Drive Applications." 22nd IEEE Workshop on Control and Modeling for Power Electronics COMPEL 2021.

As Published: https://electricayelectronica.uniandes.edu.co/sites/default/files/COMPEL%202021/22nd%20IEEE%20Workshop_%20.pdf

Publisher: IEEE

Persistent URL: <https://hdl.handle.net/1721.1/138252>

Version: Author's final manuscript: final author's manuscript post peer review, without publisher's formatting or copy editing

Terms of use: Creative Commons Attribution-Noncommercial-Share Alike



Comparison of Inverter Topologies for High-Speed Motor Drive Applications

Mohammad M. Qasim, David M. Otten, Jeffrey H. Lang, James L. Kirtley, and David J. Perreault

Massachusetts Institute of Technology

Cambridge, MA, USA

{mqasim, otten, lang, kirtley, djperrea}@mit.edu

Abstract—This paper investigates and compares the performance of three-phase inverters and sets of single-phase full-bridge inverters for motor drive applications. Comparisons are made for a given semiconductor device area and equal rms phase current ripple and the regions of the design space in which each topology is advantageous are identified. It is found that separate full-bridge inverters are preferable for designs in which switching losses are dominant, whereas three-phase inverters are preferable for designs in which conduction losses are dominant. This result suggests that individual phase drive is desirable in applications requiring high switching frequencies, as in high-speed, low-inductance machines.

Index Terms—High-speed machines, low-inductance machines, inverter, H-bridge inverter, full-bridge inverter, three-phase inverter, polyphase inverter, open-ended windings, delta-connected winding, star/Y-connected winding.

I. INTRODUCTION

Two-level inverter configurations that can be used in three-phase motor drive systems include the three-phase bridge inverter and three independent sets of single-phase full-bridge inverters, with the former being far more common [1]. While it is commonly accepted that three-phase inverters are preferable in most applications, the relative performance of these two topologies for unusual applications such as high-speed drives has not been fully established.

One effort to compare a three-phase inverter drive connected to a Y-connected machine to the full-bridge drive for a machine with open-ended windings, has been made in [2]. It was found that sets of full-bridge inverters driving the open-ended winding machine were superior in terms of inverter efficiency under equal silicon area (using IGBTs). However, the comparison was not made at equal current ripple percentage, or equivalently, equal performance and ac ripple imposed on the machine. Therefore, it does not provide a definitive comparison between the two design choices.

This paper provides a loss comparison between three-phase and full-bridge inverters for a given semiconductor device area and an equal high-frequency ripple imposed on the machine (a specified rms current ripple percentage) to identify the design regions in which each topology excels. We also provide an example illustrating that for some designs, a drive with multiple sets of full-bridge inverters is preferable from an efficiency perspective.

II. LOSS COMPARISON FOR A GIVEN SEMICONDUCTOR DEVICE AREA

In this section, we provide a generalized loss comparison between a three-phase inverter and sets of separate single-phase full-bridge (H-bridge) inverters for a given semiconductor device area. The performance metric is loss, including device conduction and switching losses.

A. Two-level Converter Topologies

Fig. 1a shows the structure of a three-phase drive system in which each phase winding is driven by a separate full-bridge inverter. Fig. 1b shows the structure of a system in which a three-phase inverter supplies a delta-connected electric machine.

These two systems may be directly compared with the same electrical machine winding (i.e., without needing to rescale machine voltages and currents by changing the numbers of winding turns). To first order, a three-phase inverter with a Y-connected machine will provide identical results as a delta-connected machine, provided the machine is rewound with an appropriate number of turns and wire gauge (i.e., providing suitable voltage and current scaling based on the well-known delta-to-wye transform). The comparison between individual-phase drive and three-phase inverter drive may thus be regarded as general.

Each full-bridge inverter consists of two half-bridges, whereas each three-phase inverter consists of three half-bridges. We focus on comparing configurations using the same total semiconductor device area (representing the same total device conductance and total device capacitance). As will be described, we also focus on comparing designs at identical phase-current ripple and dc bus voltage.

B. Conduction Loss

Consider a unit device with on-state resistance R_{on} . Let the number of devices connected in parallel per switch position be N_{FB} and N_{3PH} for the full-bridge and three-phase inverters, respectively. Additionally, let the peak fundamental-frequency phase current in each single-phase load be I_a and the peak line current for the delta-connected three-phase system be $I_{L,a}$ where $I_{L,a} = \sqrt{3}I_a$ for the same system power (i.e., the phase current magnitude for the delta-connected load is equal to that of the single-phase load, $|I_a|$). For equal total device area ($2N_{FB} = N_{3PH}$), the total equivalent on-state

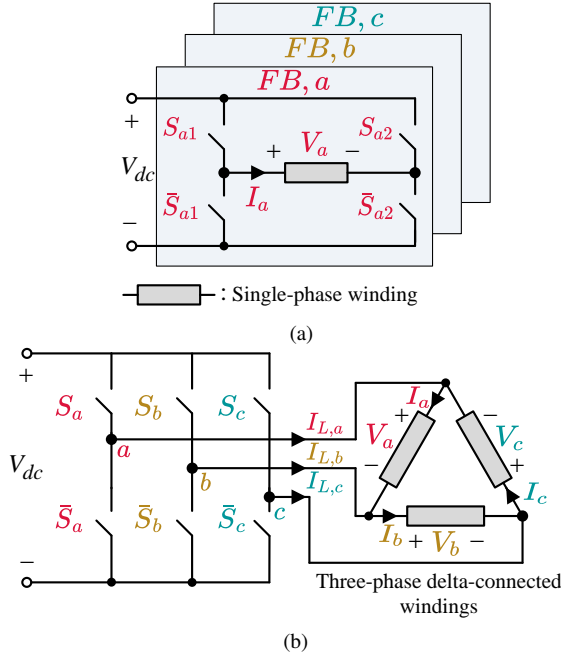


Fig. 1: Inverter structures for three-phase drives: (a) a set of three single-phase full-bridge inverters with common dc bus voltage at their input supplying three, independent single-phase windings of an open-ended winding machine; and (b) a three-phase inverter supplying a three-phase delta connected machine.

resistance through which the load current flows is $2R_{on}/N_{FB}$ for the full-bridge inverter. The total conduction loss for the full-bridge inverter is thus:

$$P_{cond,FB} = \frac{3}{2} \left(\frac{2R_{on}}{N_{FB}} \right) I_a^2 \quad (1)$$

For an equal semiconductor device area ($2N_{FB} = N_{3PH}$), the total device conduction loss for three-phase inverter at the same fundamental-frequency phase voltage and current is:

$$P_{cond,3PH} = \frac{3}{2} \left(\frac{R_{on}}{2N_{FB}} \right) (\sqrt{3}I_a)^2 \quad (2)$$

Thus,
$$\frac{P_{cond,3PH}}{P_{cond,FB}} = \frac{3}{4}. \quad (3)$$

The relation in (3) indicates that a three-phase bridge inverter is preferable to three full-bridge inverters in terms of conduction loss. This is why three-phase inverters are often preferred. However, to make a full performance comparison between these configurations, one should compare total loss, which includes both conduction and switching losses.

C. Switching Loss

Here we find the relative switching losses that may be expected in the three full-bridge and three-phase bridge cases. First, we provide the average switching loss in one device per switch position, which is developed in detail in Appendix A. Then, we compute the relative total device switching loss between full-bridge and three-phase motor drives for equivalent rms phase current ripple.

The switching loss in a bridge leg (half-bridge) over a switching cycle comprises the turn-on and turn-off losses in the active (positive-current-carrying) and freewheeling (negative-current-carrying) devices, and is generally highly dominated by the active device. For this reason, only active device switching loss characteristics are presented in most manufacturer datasheets. The total switching loss in a bridge leg can be estimated as some factor between 1 and 2 times the active device switching loss. We will refer to this loss factor as k_l . For each of the topologies under consideration, we can estimate the switching loss in a bridge leg as k_l times that modeled for the active device in the leg. In our particular experimental system with an example device from CREE, k_l has been measured to be approximately 1.3, so we use this value in the presented example. The effect of this approximation is identical in both the three-phase and three single-phase inverters cases, and does not change the overall comparison.

Considering the defined loss factor above, we can find the switching loss in each motor drive. For the three single-phase full-bridge inverters, there are two half-bridges in each full-bridge. In each half-bridge, there is one active switch and one freewheeling switch, and the total device switching loss in the half-bridge is k_l times the active device loss. Assuming N_{FB} devices per switch position, the total switching loss for three full-bridge inverters (i.e. six bridge legs) can be expressed as:

$$P_{sw,FB}^{tot} = 3 \times 2 \times k_l \times P_{sw,FB}^{1dev} \times N_{FB} \\ = 6 \times k_l \times N_{FB} \times \bar{E}_{sw,FB}^{1dev} \times f_{sw,FB} \quad (4)$$

where $P_{sw,FB}^{1dev}$ is the line-cycle average switching power loss in a single active device in a full-bridge, $\bar{E}_{sw,FB}^{1dev}$ is the line-cycle average switching energy loss in a unit active device in a full-bridge, and $f_{sw,FB}$ is the device average switching frequency of the full-bridge drive. In contrast, for the three-phase inverter (i.e. three bridge legs) with N_{3PH} devices per switch position, the total switching loss can be expressed as

$$P_{sw,3PH}^{tot} = 3 \times k_l \times P_{sw,3PH}^{1dev} \times N_{3PH} \\ = 3 \times k_l \times N_{3PH} \times \bar{E}_{sw,3PH}^{1dev} \times f_{sw,3PH} \quad (5)$$

where $P_{sw,3PH}^{1dev}$ is the line-cycle average switching power loss in a single active device in a three-phase bridge, $\bar{E}_{sw,3PH}^{1dev}$ is the line-cycle average switching energy loss in a unit active device in one half-bridge of the three-phase bridge, and $f_{sw,3PH}$ is the device average switching frequency of the three-phase drive.

For equal semiconductor device area or $N_{3PH} = 2N_{FB}$, the ratio of switching loss between the three-phase phase inverter drive and full-bridge inverter drive can be expressed as,

$$\frac{P_{sw,3PH}^{tot}}{P_{sw,FB}^{tot}} = \frac{\bar{E}_{sw,3PH}^{1dev} f_{sw,3PH}}{\bar{E}_{sw,FB}^{1dev} f_{sw,FB}}. \quad (6)$$

In (6), $\frac{\bar{E}_{sw,3PH}^{1dev}}{\bar{E}_{sw,FB}^{1dev}}$ represents the average unit-device switching energy loss of the three-phase bridge to the full bridges over a fundamental line cycle (refer to Appendix A for the estimation of device switching loss averaged over a line cycle). For

identical total device area in the two configurations, this ratio is also equivalent to the ratio of the total average switching loss energy per switching cycle in the three-phase bridge to that in the full bridges.

As shown in Appendix A, the ratio of the unit-device average switching energy loss between the three-phase drive and full-bridge drive varies between $\sqrt{3}/2$ and unity. At practical device semiconductor areas/currents, the corresponding $\frac{\bar{E}_{sw,3PH}^{1dev}}{\bar{E}_{sw,FB}^{1dev}}$ ratios approaches unity. It can be inferred, therefore, that the ratio of device average switching frequency between the three-phase and full-bridge motor drives required for equal rms phase current ripple is the dominant factor in determining the switching loss ratio in (6). In the next section, we will find the switching frequency ratio between the considered motor drives for equivalent modulation scheme, equal phase current rms ripple, and equal dc bus voltage.

III. DEVICE AVERAGE SWITCHING FREQUENCY FOR EQUAL RMS CURRENT RIPPLE

To make a fair comparison of the switching loss performance of the two topologies, we find the device average switching frequency required to achieve a specified percentage rms ripple in the machine phase currents. To make this comparison, we consider fixed-switching frequency (carrier) PWM techniques for both topologies. Specifically, three-level sine-triangle PWM modulation is used in the full-bridge drive, whereas three-level PWM with triangular carrier and one-sixth third harmonic injected references is used for the three-phase drive. It is worth noting that equivalent variable-frequency hysteretic current control techniques can also be utilized to perform the comparison and yield similar results.

A. Modulation Schemes

The well known carrier-based sine-triangle PWM and third-harmonic-injected-reference-triangle PWM techniques are used to realize equivalent three-level modulation of the full-bridge and three-phase inverters, respectively. The sine-triangle PWM for the three, single-phase full-bridge inverters and the third harmonic injected references modulation scheme for the three-phase inverter are shown in Figs. 2 and 3, respectively.

In both schemes, the duty cycle (reference) waveforms (depicted by $d_a(t)$, $d_b(t)$ and $d_c(t)$ in Fig. 2 for the three full-bridge inverters and by $\hat{d}_a(t)$, $\hat{d}_b(t)$, and $\hat{d}_c(t)$ for the three-phase inverter) are compared with a triangular carrier to generate the switching gate signals to the respective converters. In the full-bridge drive system, three cosines/sines that are 120° apart represent the modulating reference signals whereas, in the three-phase inverter, waveforms that are generated by one-sixth third harmonic injection into the three 120° apart cosines/sines represent the modulating reference signals (see reference generation in Fig. 3). For the full-bridge inverter with sine-triangle PWM (Fig. 2), the amplitude of the reference

waveforms known as the amplitude modulation index M_a can be expressed as:

$$M_a = \frac{V_a}{V_{dc}} \quad 0 < M_a < 1 \quad (7)$$

where V_a is the fundamental peak terminal voltage. For the three-phase inverter with third-harmonic-injected-reference-triangle PWM (Fig. 3), the modulation index extends to $2/\sqrt{3}$ so that the injected-3rd-harmonic instantaneous reference waveforms do not exceed unity in amplitude (i.e., stays in linear modulation regime without stepping into over-modulation) and can be expressed as,

$$\hat{M}_a = \frac{2}{\sqrt{3}} \frac{V_a}{V_{dc}} = \frac{2}{\sqrt{3}} M_a \quad 0 < \hat{M}_a < \frac{2}{\sqrt{3}} \quad (8)$$

B. Switching Frequency Ratio for Equal RMS Current Ripple

As developed in [3], the rms of the output current ripple waveform ($I_{ripple,rms}$ or $rms(i_{ripple}(t))$) for the considered single-phase and three-phase converter topologies can be found given the output ripple switching period $T_{FB,3PH}$, the phase inductance of the machine L_a , the applied dc bus voltage V_{dc} , and a factor $h(M_a)_{FB,3PH}$ —known as the harmonic distortion factor (HDF). This factor depends on the PWM modulation scheme and is usually expressed as a function of the amplitude modulation index. Correspondingly, the output ripple frequencies of the full-bridge drive and three-phase drive (f_{FB} and f_{3PH}) can be expressed as:

$$f_{FB} = 2f_{sw,FB} = \frac{V_{dc}}{L_a I_{ripple,rms}} \sqrt{\frac{h(M_a)_{FB}}{48}} \quad (9)$$

$$f_{3PH} = 2f_{sw,3PH} = \frac{V_{dc}}{L_a I_{ripple,rms}} \sqrt{\frac{h(M_a)_{3PH}}{48}} \quad (10)$$

The harmonic distortion factors in (9) and (10) for the respective full-bridge inverter with three-level sine-triangle pwm, and for the three-phase inverter with third-harmonic-injected-reference-triangle pwm are provided in Appendix B. For three-level modulation schemes, the device average switching frequency (carrier frequency of the triangle waveform) is half the ripple frequency ($f_{sw,FB} = 1/2f_{FB}$ and $f_{sw,3PH} = 1/2f_{3PH}$). Also, in (9) and (10), equal phase current rms ripple, $I_{ripple,rms}$, equal phase inductance, L_a , and equal dc bus voltage, V_{dc} , are considered for both topologies.

The ratio of switching frequency between the three-phase inverter and the full-bridge inverter as a function of the modulation index (required for a given machine phase voltage and current ripple under the discussed three-level modulation schemes) can thus be expressed as:

$$\begin{aligned} \frac{f_{sw,3PH}}{f_{sw,FB}} &= \sqrt{\frac{h(M_a)_{3PH}}{h(M_a)_{FB}}} = F(M_a) \\ &= \sqrt{\frac{2M_a^2 - \frac{32}{3\pi}M_a^3 + \frac{16}{9}M_a^4}{2M_a^2 - \frac{32}{3\pi}M_a^3 + \frac{3}{2}M_a^4}} \quad 0 < M_a < 1 \quad (11) \end{aligned}$$

The ratio in (11) is plotted in Fig. 4 as a function of the modulation index M_a . Overall, the ratio is always > 1 for the entire modulation index range, which suggests that the three-phase inverter always requires higher switching frequency than the full-bridge motor drive for equal rms current ripple. It can also be highlighted that the switching frequency ratio is close to unity at low modulation indices {e.g. at $F(M_a \in [10^{-4} \ 0.5]) \in [0 \ 1.05]$ }. From 0.6 to unity modulation index, the frequency ratio varies from 110% to 191%, indicating that the required device switching frequency for the three-phase inverter relative to that of the single-phase inverters increases with higher modulation indices. For example, the three-phase inverter switching frequency is almost twice that of the full-bridge inverter at unity modulation index. The relation in (11) and Fig. 4 is important because it indicates that three single-phase full-bridge inverters require substantially lower switching frequency than a three-phase bridge for equal phase current rms ripple.

Considering (6), in which the first factor is close to unity, and the second factor is represented in Fig. 4, it may be concluded that for most cases of interest (i.e., at high modulation index) the switching losses in a three-phase bridge are considerably higher than that for a set of single-phase bridges for equivalent rms phase-current ripple. Therefore, single-phase drives have an efficiency edge over three-phase bridge drives when operating in a regime in which the converter total device losses are dominated by the switching losses.

IV. MOTOR DRIVE EXAMPLE

Here we illustrate a design in which there is a significant advantage to using three single-phase inverters over a three-phase inverter. The system parameters of a 3.6 kW three-phase, high-speed motor drive operating at 2 kHz drive frequency and 3.13% rms phase current ripple are summarized in Table I. The example design is for a sinusoidal back-emf voltage, such as in some permanent magnet synchronous motors (PMSMs).

Substituting the example parameters in (9)-(11), for 3.13% rms phase current ripple, the required switching frequency for the three-phase inverter and full-bridge inverter for the example modulation index of 0.9215 are 110 kHz and 68 kHz, respectively, or a frequency ratio of ~ 1.62 .

A. Motor Drive Simulation Results

Here we use simulation to validate the analytical results for the required switching frequencies of the three-phase inverter and full-bridge inverter in the context of our example. The full-bridge drive is implemented with sine-triangle PWM, whereas the three-phase drive is implemented with third-harmonic-injected-reference-triangle PWM (as shown in Section III-A). In case of the full-bridge motor drive, the load is simulated by three separate single-phase windings¹, whereas it is simulated with three single-phase windings connected in delta to make up the three-phase load for the three-phase drive.

¹E.g. In machines with open-ended windings, both ends of all three windings are accessible for the desired connection configuration.

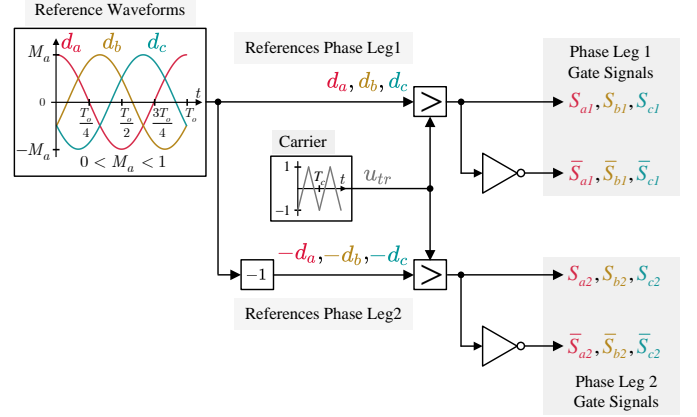


Fig. 2: Sine-triangle PWM three-level modulation scheme for the full-bridge inverter.

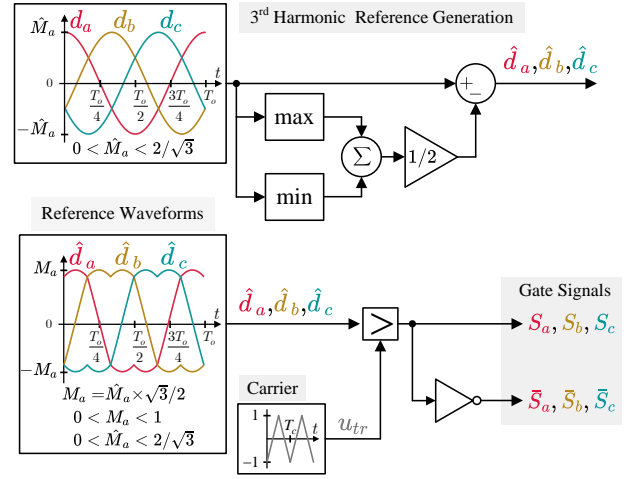


Fig. 3: Third-harmonic-injected-reference PWM three-level modulation scheme for the three-phase inverter.

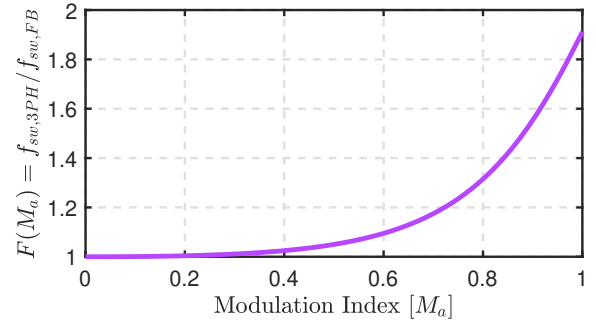


Fig. 4: Ratio of device switching frequency required between the three-phase drive and single-phase drive as a function of M_a ($0 < M_a \leq 1$), for equal phase voltage and rms phase current ripple.

TABLE I: Example parameters of a **3.6 kW** three-phase motor drive system to achieve **3.13%** rms phase current ripple

$P_{o,tot}$ Output power [kW]	V_{dc} DC bus voltage [V]	f_o Drive frequency [kHz]	E_a O.C./EMF voltage [V]	V_a Phase voltage [V]
3.6	720	2	641.4	663.5
I_a Phase current [A]	L_a Phase induc. [mH]	R_a Phase resis. [Ω]	M_a Mod. index [-]	$I_{ripple,rms}$ rms curr. ripple [A]
3.742	3.2	1.2	0.9215	0.0828 (3.13% $\frac{I_a}{\sqrt{2}}$)

The full-bridge and three-phase drives are simulated with carrier frequencies of 68 kHz and 110 kHz, respectively. The simulated full-bridge and three-phase drive waveforms are shown in Figs. 5 and 6, respectively.

The modulation reference waveforms reflect a modulation index of $M = 0.9215$ for the full-bridge system or $\hat{M} = 2/\sqrt{3}M = 2/\sqrt{3} \cdot 0.9215 = 1.064$ for the three-phase delta-connected system (Figs. 5a and 6a). From Figs. 5b-5d and 6b-6d, the phase currents and fundamental output voltage for the full-bridge drive and the three-phase drive have amplitudes consistent with the system parameters given in Table I. The rms values of the switching ripple phase current of the full-bridge drive and three-phase drive (Figs. 5e and 6e) are 0.0829 A and 0.0821 A, respectively (less than 1% percentage difference between the the full-bridge drive and three-phase inverter drive). This matches the phase current rms ripple predicted in (9) and (10) for the full-bridge and three-phase drives, respectively.

B. Total Device Loss Versus Semiconductor Device Area

To quantify the loss comparison, a design study based on device semiconductor area is carried out using SiC power MOSFETs as an example device. To provide an idealized performance comparison, we consider an arbitrarily-scalable semiconductor device area (or number of paralleled devices) based on the characteristics of the C3M0350120J 1200 V SiC Power MOSFET from CREE as a per-unit device.

The device-measured switching loss curves provided by the manufacturer's datasheet [4] were used to calculate the device average total (turn on + turn off) switching loss for a sinusoidal current over the fundamental drive cycle as explained in Section II-C (interpolating on datasheet loss curves across voltage to compute switching loss). The switching loss ratio between the three-phase drive and full-bridge drive for equal normalized device semiconductor area (or total number of C3M0350120J devices) is shown in Fig. 7. It can be seen from the figure that the switching loss ratio varies between 0.89 and 0.98 falling between the theoretical limits provided in Section

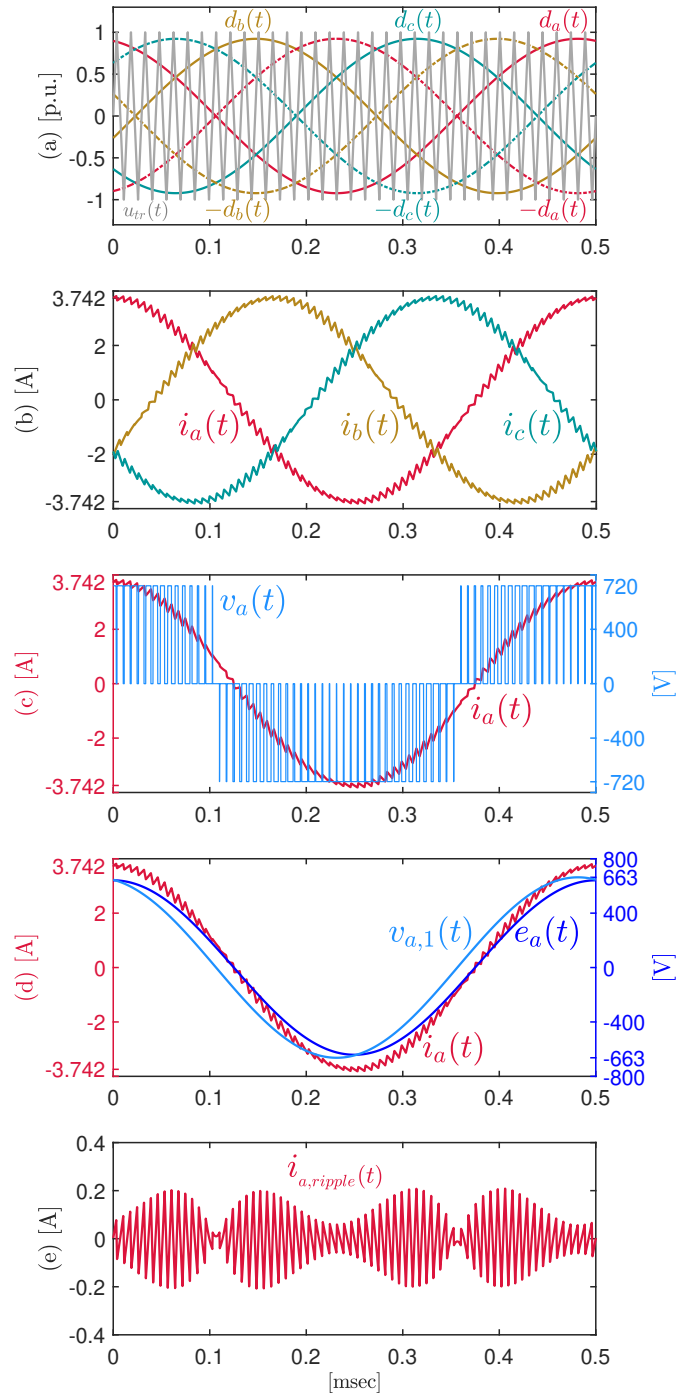


Fig. 5: Simulation waveforms of the full-bridge motor drive with sine-triangle PWM, $M = 0.9215$ and $f_{c,FB}/f_o = 34$. Waveforms shown from top to bottom are (a) the $f_o = 2$ kHz reference waveforms as compared to the 68 kHz triangle carrier, (b) phase currents, (c) phase-a current and phase-a output voltage, (d) phase-a current, fundamental-frequency output voltage and back-emf voltage, and (e) phase-a ripple current waveform with rms value 0.0829 A ($\sim 3.13\%$ of rms phase current).

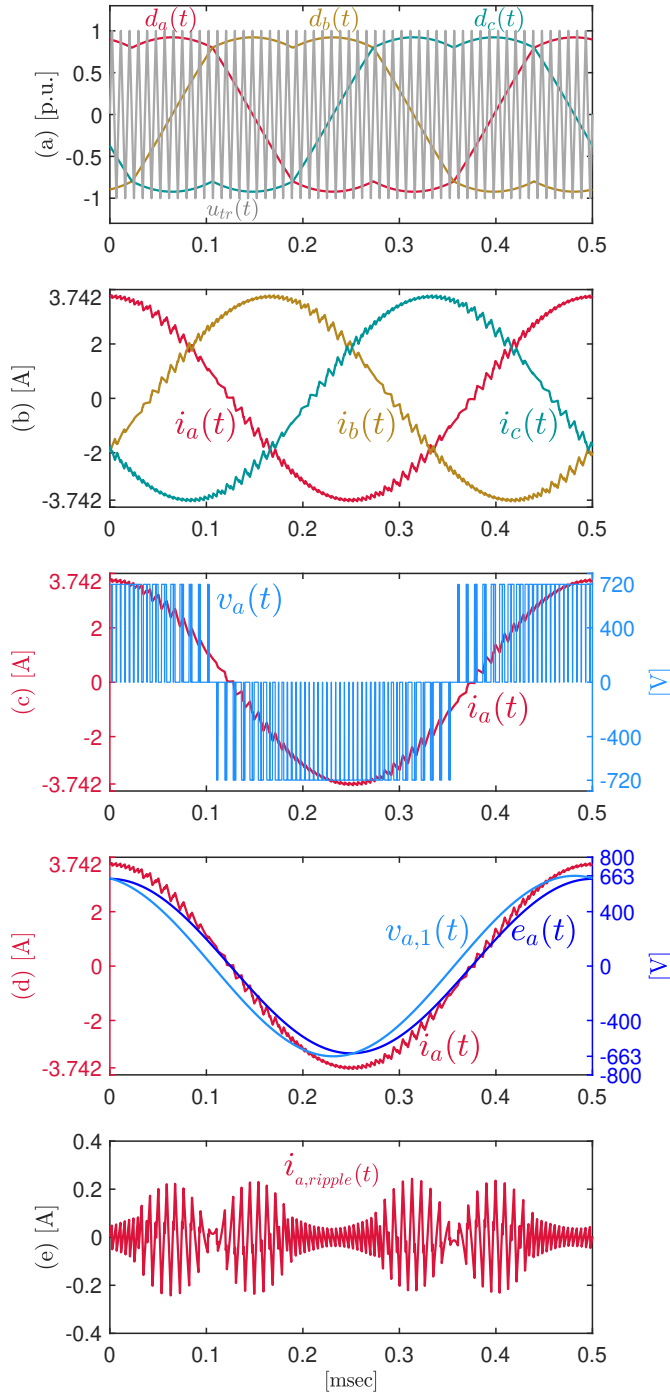


Fig. 6: Simulation waveforms of the three-phase motor drive with third-harmonic-injected-reference-triangle PWM, $M = 0.9215$ and $f_{c,FB}/f_o = 55$. Waveforms shown from top to bottom are (a) the $f_o = 2$ kHz third-harmonic-injected-reference waveforms as compared to the 110 kHz triangle carrier, (b) phase currents, (c) phase-a current and phase-a output voltage, (d) phase-a current, fundamental-frequency output voltage and back-emf voltage, and (e) phase-a ripple current waveform with rms value 0.0821 A ($\sim 3.10\%$ of rms phase current).

II-C (refer to (19) in Appendix A for detailed discussion). The higher switching loss of the three-phase bridge is thus due to the much higher switching frequency required to achieve the specified rms phase current ripple.

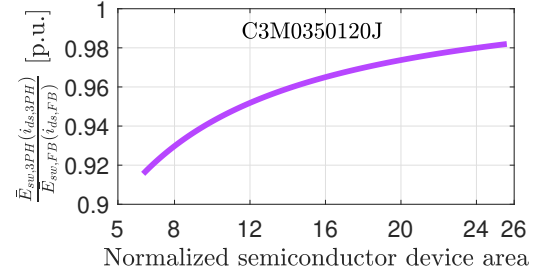


Fig. 7: The curve shows the device average switching energy loss ratio between the three-phase drive and the full-bridge drive versus the normalized semiconductor device area (or total number of C3M0350120J devices) over a switching cycle at rated operation.

Using the analytical model and calculations developed in the preceding sections (device loss in Sections II-B and II-C), and switching frequency ratio for equal rms ripple current and phase voltage in Sections III-B and IV-A, the total device loss (conduction plus switching) versus normalized device area are calculated as shown in Fig. 8a-8c².

If the full-bridge and three-phase inverters were each to be built at their optimum loss points (14.2 & 9.7 per unit of device area, respectively), the full-bridge inverter would have 12.21% lower device losses than the three-phase bridge inverter. Furthermore, the full-bridge drive could be built at the optimum point of the three-phase inverter (same device area), and yet result in less loss (since the three-phase inverter optimum point is in the switching loss dominant region).

The above comparison is for a continuously-scalable semiconductor die area which is not realizable in practice due to device quantization. To translate this arbitrarily-scalable die area into an actual number of C3M0350120J MOSFETs, we compare the two topologies for near-optimum designs based on equal C3M0350120J total device area comprising 12 MOSFETs in total. This represents one device per switch position ($N_{FB} = 1$) for the three full-bridge inverter drive, and two paralleled devices per switch position ($N_{3PH} = 2$) for the three-phase inverter drive. In this case, the full-bridge drive system still excels in performance with 12.75% lower total device losses than the three-phase bridge drive. From an efficiency perspective, the full-bridge drive is thus preferable to the three-phase drive in this example design.

V. CONCLUSION

This work compares the performance of two-level inverter topologies for motor drive applications. The study uses analytical loss modeling and is verified by computer simulations. The outcome of this comparison shows that for a

²The first point on the left side of each loss curve represents a conceptual thermal limit on minimum semiconductor device area.

given semiconductor device area and equal rms phase current ripple, single-phase full-bridge based motor drive systems have efficiency benefits over three-phase inverters in designs where the switching losses are dominant such as occurs for driving low-inductance, high-speed electric machines.

APPENDIX A DEVICE SWITCHING ENERGY LOSS CALCULATION

In this appendix, we develop the calculation of the average device switching energy E_{sw}^{1dev} from the switching loss energy curve of some active switching device (provided in the device datasheet information or obtained by simulation or experimental measurement). Assuming a sinusoidal output phase current of the motor drives considered, the instantaneous on-state current in a switch is equal to the phase current in the full-bridge inverter, or,

$$i_{FB} = I_a \cos(2\pi f_o t) \quad (12)$$

whereas, in the three-phase inverter the instantaneous current flowing in a switch is the line current,

$$i_{3PH} = I_{L,a} \cos(2\pi f_o t). \quad (13)$$

In (12), (13), f_o is the fundamental line (drive) frequency.

If there are ‘ n ’ parallel devices per switch position, then the current in one device per switch position for the full-bridge and three phase drives are:

$$i_{FB,1dev} = i_{FB}/n = \frac{I_a}{n} \cos(2\pi f_o t), \quad (14)$$

$$i_{3PH,1dev} = i_{3PH}/n = \frac{I_a}{n} \cos(2\pi f_o t). \quad (15)$$

In (14), ‘ n ’ indicates any number of devices per switch position and can be non-integer for scalable semiconductor device area. Equivalently, ‘ n ’ can be regarded as a scaling factor of semiconductor device area. For the purpose of comparing the converters under equal semiconductor device area, let $n = N_{FB}$ for the motor drive comprising three, single-phase full-bridge inverters and $n = N_{3PH}$ (or $n = 2N_{FB}$ for equal semiconductor device area) for the three-phase inverter motor drive.

In view of the individual device currents defined above, we can define the sum of the turn-on and turn-off, instantaneous switching energy loss for an individual (active) switching device in one half-bridge as $e_{sw,k}(i_{k,1dev}, v_{sw})$ in which $i_{k,1dev}$ is the current in one device per switch position for the corresponding full-bridge (FB) inverter and three-phase bridge inverter (3PH), respectively (abbreviated by $k=\{FB,3PH\}$). The individual switching device energy loss $e_{sw,k}$ is characteristic of a given device and is a monotonically increasing function of the device current that can be obtained based on the device datasheet information, simulation, or experimental measurement.

Now that the instantaneous switching energy loss is defined, we can find the device average switching loss for carrier-based pwm inverters where the carrier or device average switching frequency is fixed and assuming that the switching cycle is

considerably shorter than the fundamental line (drive) cycle. The average switching loss ($P_{sw,k}$) for one device per switch position per phase for a given dc bus voltage V_{dc} over a fundamental line cycle, for the respective full-bridge drive and three-phase drive, can thus be expressed as:

$$\begin{aligned} P_{sw,k}^{1dev} &= \frac{2}{T_o} \int_0^{\frac{T_o}{2}} e_{sw,k}(|i_{k,1dev}|, V_{dc}) f_{sw,k} dt \\ &= f_{sw,k} \frac{2}{T_o} \int_0^{\frac{T_o}{2}} e_{sw,k}(|i_{k,1dev}|, V_{dc}) dt \\ &= f_{sw,k} \langle e_{sw,k}(|i_{k,1dev}|, V_{dc}) \rangle_{T_o} = f_{sw,k} \bar{E}_{sw,k}^{1dev}. \end{aligned} \quad (16a)$$

Since the switching loss energy is monotonic with $|i_{k,1dev}|$ and may be approximated as affine with $|i_{k,1dev}|$, we can approximate $\langle e_{sw,k}(|i_{k,1dev}|, V_{dc}) \rangle_{T_o}$ as $e_{sw,k}(|i_{k,1dev}|_{T_o}, V_{dc})$. This approximation becomes exact if $e_{sw,k}$ is exactly affine with $i_{k,1dev}$. The relation in (16a) can thus be alternatively expressed as,

$$\begin{aligned} P_{sw,k}^{1dev} &= f_{sw,k} \bar{E}_{sw,k}^{1dev} \approx f_{sw,k} e_{sw,k}(|i_{k,1dev}|_{T_o}, V_{dc}) \\ &= f_{sw,k} e_{sw,k} \left(\frac{2}{\pi} \frac{I_k}{n}, V_{dc} \right) \end{aligned} \quad (16b)$$

Let us find the limits of the relative device switching energy loss between the the three-phase and full-bridge motor drives. Given the monotonicity behaviour of the switching energy loss with the device instantaneous current i_k , we can express it as an n^{th} order polynomial or $e_{sw,k}(i_k, v_{sw}) = \alpha_0 + \alpha_1 i_k + \alpha_2 i_k^2 + \dots + \alpha_n i_k^n$, $\alpha'_s > 0$. For the purpose of finding the limits of the relative device switching energy loss, it is justifiable to assume the first order Taylor series approximation would be a sufficient representation of the device switching energy loss. Applying this expression to the switching energy loss for one device per switch in (16) for the considered three-phase and full-bridge motor drives we get,

$$\begin{aligned} \bar{E}_{sw,3PH}^{1dev} &= \alpha_1 \frac{\sqrt{3} I_a}{2 N_{FB}} + \alpha_0 \\ &= \begin{cases} \alpha_0 & \frac{I_a}{N_{FB}} \ll \alpha_0 \quad (N_{FB} \rightarrow \infty) \\ \alpha_1 \frac{\sqrt{3} I_a}{2 N_{FB}} & \frac{I_a}{N_{FB}} \gg \alpha_0 \quad (N_{FB} = 1, I_a \rightarrow \infty) \end{cases} \end{aligned} \quad (17)$$

$$\begin{aligned} \bar{E}_{sw,FB}^{1dev} &= \alpha_1 \frac{I_a}{N_{FB}} + \alpha_0 \\ &= \begin{cases} \alpha_0 & \frac{I_a}{N_{FB}} \ll \alpha_0 \quad (N_{FB} \rightarrow \infty) \\ \alpha_1 \frac{I_a}{N_{FB}} & \frac{I_a}{N_{FB}} \gg \alpha_0 \quad (N_{FB} = 1, I_a \rightarrow \infty) \end{cases} \end{aligned} \quad (18)$$

Substituting (17) and (18) in the switching energy loss ratio in (6), we can approximate the limits of the relative device average switching energy loss between the three-phase inverter drive and the drive consisting of three full-bridge inverters as,

$$\sqrt{3}/2 < \frac{\bar{E}_{sw,3PH}^{1dev}}{\bar{E}_{sw,FB}^{1dev}} < 1 \quad \infty > \frac{I_a}{N_{FB}} > 0 \quad (19)$$

From (19), the device average switching energy loss ratio

between the three-phase inverter drive and full-bridge drive approaches unity with small currents or large semiconductor device area, whereas it goes to $\sqrt{3}/2$ if we scale down the device area to a small value (i.e., large device current).

APPENDIX B HARMONIC DISTORTION FACTORS

As developed in [3], the HDFs $h(M_a)_{FB}$ and $h(\hat{M}_a)_{3PH}$ for the full-bridge drive and three-phase inverter drive with the chosen three-level modulation schemes may be expressed as:

$$h(M_a)_{FB} = 2M_a^2 - \frac{32}{3\pi}M_a^3 + \frac{3}{2}M_a^4 \quad 0 < M_a < 1 \quad (20)$$

and,

$$h(\hat{M}_a)_{3PH} = \frac{3}{2}\hat{M}_a^2 - \frac{4\sqrt{3}}{\pi}\hat{M}_a^3 + \hat{M}_a^4 \quad 0 < \hat{M}_a < 2/\sqrt{3}. \quad (21)$$

Comparing (7) to (8), shows that for a given dc voltage bus and machine terminal inductance, the modulation index ought to be higher for the three-phase inverter to achieve the same phase voltage and rms phase current ripple as the single-phase inverter. For instance, the peak fundamental voltage is equal to the dc bus voltage when the modulation index is unity for the full-bridge drive but has to extend to $2/\sqrt{3}$ (≈ 1.15) for the three-phase drive without stepping into over-modulation. Under the assumption of equal phase voltage and rms current ripple, it is therefore reasonable to compare the HDFs for both converters with respect to the same modulation index M_a . Thus, we can express the HDF for the three-phase bridge inverter in terms of M_a as:

$$\begin{aligned} h(M_a)_{3PH} &= \frac{3}{2}\left(\frac{2}{\sqrt{3}}M_a\right)^2 - \frac{4\sqrt{3}}{\pi}\left(\frac{2}{\sqrt{3}}M_a\right)^3 + \left(\frac{2}{\sqrt{3}}M_a\right)^4 \\ &= 2M_a^2 - \frac{32}{3\pi}M_a^3 + \frac{16}{9}M_a^4 \quad 0 < M_a < 1 \quad (22) \end{aligned}$$

It can be observed that all the terms in (22) of the three-phase inverter are exactly the same as the full-bridge inverter except the last term. It can be noticed that the last term, $\frac{16}{9}M_a^4$ or $1.7\bar{7}M_a^4$, in the three-phase system, is larger than $1.5M_a^4$ of the single-phase system, which indicates higher HDF for equal phase voltage and rms current ripple.

REFERENCES

- [1] J. Kassakian, M. Schlecht, and G. Verghese, "Variable-Frequency dc/ac Converters," in *Principles of Power Electronics*. Boston, MA, USA: Addison-Wesley, 1991, ch. 8, pp. 167–196.
- [2] M. Neubert, S. Koschik, and R. W. De Doncker, "Performance comparison of inverter and drive configurations with open-end and star-connected windings," in *2014 International Power Electronics Conference (IPEC-Hiroshima 2014 - ECCE ASIA)*, 2014, pp. 3145–3152.
- [3] D. G. Holmes and T. A. Lipo, *Pulse Width Modulation for Power Converters: Principles and Practice*, 2003, ch. 4.3 & 5.4, pp. 169–177, 241–249.
- [4] *C3M0350120J Silicon Carbide MOSFET*, CREE, 2020, Rev. A.

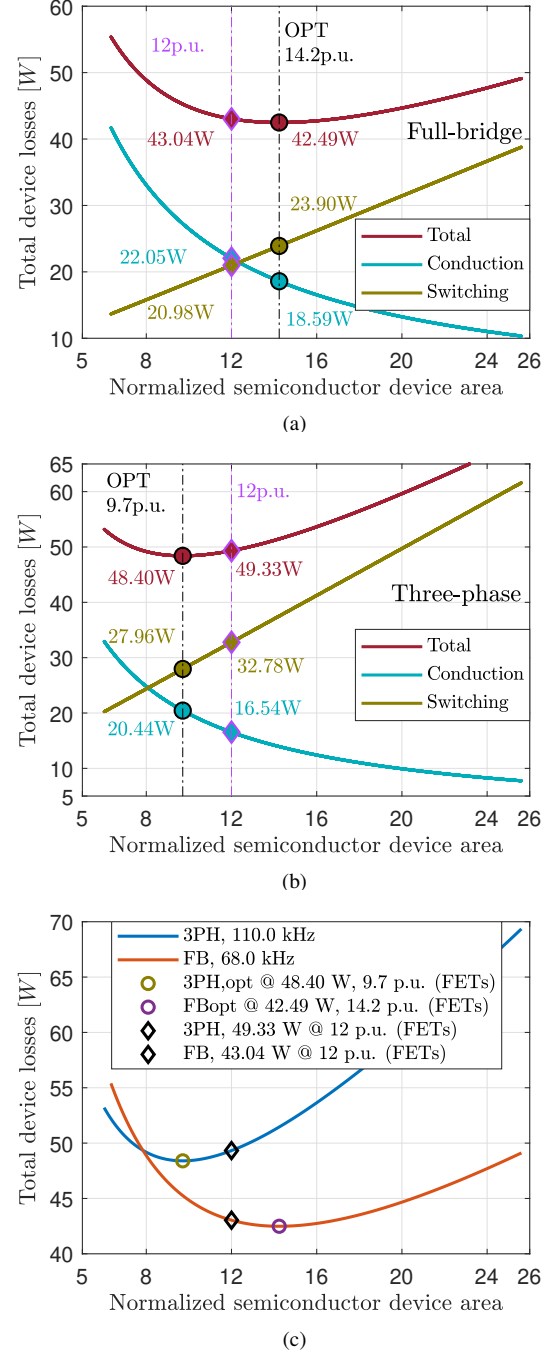


Fig. 8: Conduction, switching, and total losses vs. normalized device area calculated for 68kHz and 110kHz device switching frequencies for the respective (a) set of three single-phase full-bridge inverters and (b) three-phase inverter. In (c) the total device losses (conduction plus switching losses) vs. normalized device area for both the full-bridge and three-phase inverter motor drives are depicted on the same plot. A normalized device area of 12 represents a set of full bridges using one C3M0350120J device per switch position or a three-phase bridge with two parallel C3M0350120J devices per switch position.